Available online at www.sciencedirect.com
SCIENCE DIRECT
Journal of Photochemistry and Photobiology A: Chemistry 179 (2006) 213–223
Journal of Photochemistry and Photobiology A:Chemistry
www.elsevier.com/locate/jphotochem

The role of nitrogen doping on the development of visible light-induced photocatalytic activity in thin TiO_2 films grown on glass by chemical vapour deposition

H.M. Yates [a,*], M.G. Nolan [a], D.W. Sheel [a], M.E. Pemble [b]

[a] *Institute for Materials Research, Cockcroft Building, University of Salford, Salford M5 4WT, UK*
[b] *Tyndall National Institute, University College Cork, Lee Maltings, Prospect Row, Cork, Ireland*

Received 23 May 2005; received in revised form 20 July 2005; accepted 12 August 2005
Available online 23 September 2005

Abstract

A brief review of the findings of a range of studies aimed at describing the influence of the N-doping of TiO_2 thin films and particles on possible visible light-induced photoactivity is presented. By way of a new approach to the direct growth of N-doped TiO_2 thin films, the physical and photochemical effects of the addition of ammonia during atmospheric chemical vapour deposition (CVD) growth of TiO_2 are described. It is found that the addition of ammonia to the CVD reactive gas mixture causes a dramatic change in film morphology and a reduction in growth rates. In addition, it is found that although we have clear evidence for the incorporation of β-substitutional N atoms within the growing film, there is no evidence of any appreciable photocatalytic activity of the doped TiO_2 films when irradiated with visible light. In fact the degradation in film morphology results in a decrease in conventional UV-induced photoactivity as compared to that for an undoped film. These findings are discussed in terms of the findings of other studies of N-doped TiO_2 films that have been reported.

Keywords: Titania; N-doping; Photoactivity; Chemical vapour deposition

1. Introduction

Heterogeneous photocatalysis is attracting extensive interest for the degradation of organic pollutants [1–6] and the production of self-cleaning [7,8] or anti-bacterial surfaces [9,10]. Much attention has been focussed on the photocatalytic activity of nanocrystalline TiO_2 powders or films under supra-bandgap ultraviolet illumination. In this reaction, UV illumination results in the photogeneration of electron–hole pairs. The electrons (conduction band) and holes (valence band) then react with surface species to produce highly oxidizing species capable of mineralizing organics adsorbed at the TiO_2 surface.

In order to observe these effects TiO_2 thin films or particles, must be irradiated with light at an energy greater than the bandgap of 3.0 eV (rutile) or 3.2 eV (anatase). Another effect of this type of irradiation is to make the TiO_2 surface become superhydrophilic, dramatically increasing the wettability of the surface and hence greatly assisting the removal of degradation products.

Despite the many potential applications of these types of materials, their use is currently limited to environments where sufficient UV light can be made to impinge upon the TiO_2 surface. Thus it has become an important goal in the development of these materials, to try to modify them such that lower energy, visible light such as conventional internal light sources, may also be used to stimulate both the photoacatalytic activity and the superhydrophilicity that usually accompanies it. With this aim in mind, there have been a number of studies aimed at modifying the TiO_2 material via doping with various moieties [11–15].

Via the inclusion of specific dopants it should be possible to improve the efficiency of the photocatalytic behaviour by creating new band structures or by suppressing the recombination of photogenerated electron–hole pairs to improve quantum efficiency. In this respect a reduction in recombination efficiency arising from enhanced charge separation may also be obtained by coupling two semiconductors with suitable conductance and valence band potentials [16].

* Corresponding author. Tel.: +44 161 295 3115; fax: +44 161 295 5111.
E-mail address: H.M.Yates@Salford.ac.uk (H.M. Yates).

1010-6030/$ – see front matter © 2005 Elsevier B.V. All rights reserved.
doi:10.1016/j.jphotochem.2005.08.018

Many authors have concluded that N-doping of TiO_2 leads to visible light photoactivity, but there is a difference in opinion as to how doping achieves this, as well as disagreements in many of the conclusions drawn from the results. Theoretical studies [17,18] modelling the density of states within the conduction band of doped TiO_2 suggest that substitution doping by N is effective because its 2p states contribute to bandgap narrowing by mixing with the O 2p states. Also, the small change of ion size from O to N reduces the disturbance in the crystal lattice, although this will still occur. That the N is substitutional is in agreement with experimental results from Irie et al. [19]. However, it is also suggested that the N should be in an interstitial site [20], or that it is due to N interstitial site bound to hydrogen [21,22]. Alternatively, it has been suggested that the photocatalytic reaction occurs via surface intermediates of O reduction or H_2O oxidation and not by direct reaction with the holes trapped at N induced mid-gap levels [23]. The formation of the O vacancies, during the nitriding process, is considered to improve the visible light activity by acting as colour centres to create absorption sites [24] or by acting as electron traps [25]. These latter phenomena occur when an electron is excited to the oxygen vacancy state from the valance band (even under visible light). These electrons (or the holes formed) react with atmospheric oxygen (or an oxygen related species) producing reactive species (O^- or atomic oxygen), which participate in the oxidation of surface species. Alternatively, the same phenomenon has been cited as possibly responsible for reducing the activity [26] as the trapped photoelectrons cannot easily reach the surface reaction sites. This last point illustrates the level of disagreement that is typical of some work in this area.

Continuing with the theme that N-doping could actually reduce activity, it is well known that doping metal oxides with other elements can lead to electronic mid-gap states associated with dopants [27]. Subsequent trapping of photogenerated holes at such mid-gap states leads to a decrease in their oxidation power. Additionally, doping may induce structural instabilities in the TiO_2, due to introduction of lattice distortions and bond weakening.

There are several other theories, which have been cited, in order to account for the reduction in activity observed following N-doping. The first of these describes the possible detrimental effects of N-doping arising from the induction of ionic charge compensation [28] as N acceptors are easily compensated by donor levels, which are related to additional O vacancies and cations, i.e. an increase in electronically reduced Ti^{3+} states. For this reason Diwald et al. have concluded that doping with substitutional N leads to a blue shift due to the partial filling of the conduction band by electrons induced by the N doping [28].

Ion bombardment, apart from the creation of defects, also leads to entrapment of N atoms in interstitial sites and hence reduced photocatalytic behaviour [22]. However, it has also been reported that Ar^+ bombardment of TiO_2 leads to preferential sputtering of O atoms with subsequent reduction of Ti^{4+} to Ti^{3+} and Ti^{2+} [29], thus dramatically changing the nature of the sample.

Finally, although no explanations are given, in their study Frach et al. [30] go as far as to state that no improvement in visible light activity was found on N-doping.

In terms of those studies that suggest that N-doping leads to an improvement in visible light photoactivity, we find that direct comparison of data is extremely difficult for two main reasons. Firstly, the methods of preparation employed leads to the production of materials that vary dramatically in terms of quality and surface area via the formation of a range of powders, films or single crystals. For example studies have resulted in materials where the film thickness has varied from 80 nm [22] to 750 nm [31]. Secondly, the methods used to test for visible light activity vary, with no standard test being employed for specific forms of TiO_2. This latter point is particularly significant, since for conventional photoactivation by UV light, identical TiO_2 samples will yield quite different rates of activity if the materials being degraded are not themselves identical [30–32]. Thus the need for some kind of standard testing is easily recognised. In the development of such a testing procedure, factors such as the variation in crystalline type, surface area, surface reactivity towards particular species (e.g. enthalpies of adsorption), the intensity and spectral profile of the light source and the sensitivity of the method used to detect photoactivity must all be considered.

The difficulties involved in this type of testing can be illustrated by considering the work of Diwald, who has shown that the photo-threshold energy could be shifted either to lower energy [21] (as also seen by Asahi et al. [17]) or to higher energy relative to the undoped sample depending on the method used to produce the doped TiO_2. However, examination of these studies reveals that the group of Diwald use certain methods of measuring the photo-threshold (O_2 photodesorption [27] and the photochemical reduction of Ag^+ ions (aq.) [21]) while the group of Asahi uses another (photo-degradation of acetaldehyde [17]). In addition, this comparison also reveals that each group used a different crystallographic form of TiO_2, thus rendering any comparison essentially invalid.

Another aspect of N-doping that should also be considered is the study by Li in which it is reported that the nature and level of activity varies depending on the nitriding compound employed [33]. However, in this paper the determination of N content was by elemental methods only as no N was detected by XPS, so the chemical state of the N could not be determined, while presumably the presence of other elements at low levels could also not be detected.

In general, the methods used to date to synthesise N-doped TiO_2 can be divided into three types:

(1) Modification of existing TiO_2 via ion bombardment [22,28].
(2) Modification of existing TiO_2 in the forms of powder [17,19,23], films [18] and single crystal [21], or TiN [34,35] via gas phase chemical impregnation.
(3) Growth of TiN_xO_y from liquid [23,36] or gaseous [37] precursors.

In this respect it is relevant to this present publication that, as far as the authors are aware, no other studies of the direct growth of N-doped TiO_2 by atmospheric CVD methods have

been reported previously, and only one other by low pressure CVD methods reported [37].

The specific methods that have been employed in order to try to detect photoactivity in the visible are numerous. In terms of assessing these approaches, it is informative to consider for example, the range of light sources that have been employed in such studies. Sources of visible light ranging from fluorescent 'daylight' tubes (6 W) [17,31], Xe arc lamps (100–350 W) [18,22,23] to high-pressure Hg lamps (500 W) [21] have been used. With these a variety of filters (cut off, band-pass, etc.) have been employed designed to restrict the wavelengths to those required, with the visible light region usually taken as >380 nm, although in at least one study, no attempts were made to filter out the possible UV components considering these to be of such small intensity as to be negligible [38]. A further problem with this particular study was the fact that the reference non-nitrided sample was the original amorphous TiO_2 powder. As such no allowance was made for the thermally induced crystallisation that would occur, simply as a result of the temperatures employed during the nitriding process. In terms of the search for visible light photoactivity, many groups [17,22,31,35] have followed the decomposition of methylene blue by monitoring changes in the absorption or transmission at specific wavelengths. Great care is needed in setting up this type of experiment in order to differentiate between fading of the dye due to photoacatalytic activity (decomposition of the dye) and reduction of the dye to the transparent form as a result of electron transfer reactions [39]. Other groups have followed the decomposition of gaseous organic compounds via gas chromatography [17,19] or photoacoustic methods [18]. Additional testing methods that have been used include the photochemical reduction of Ag^+ ions [21] via the capture of the photogenerated electrons and hence formation of metallic Ag clusters, the use of samples in the form of electrodes and the direct measurement of the photocurrent [23] and the mass spectral measurement of the photodesorption of molecular O_2 under UHV conditions [28]. These methods aside, possibly the most widely employed method of gauging photocatalytic activity, particularly for thin film TiO_2 samples, is that which studies the degradation of stearic acid [40–42]. This test is simple to set up and run, and needs no dedicated equipment beyond a standard laboratory FTIR spectrometer. Since stearic acid is a solid at room temperature it is more easily controlled than a solution or gas, while it also provides a good model for typical organic surface contamination.

In an attempt to produce a definitive study of the possible role of N-doping in TiO_2 thin films, we report here the findings of a study in which N-doping was achieved during growth of TiO_2 thin films by chemical vapour deposition (CVD). By using the CVD approach we adopt a tried and tested method for the production of highly photoactive TiO_2 so as to be able to produce a range of undoped control samples for comparison purposes. Additionally, we identify the chemical state of the dopant N atoms directly via XPS analysis. Finally, we compare sample morphology, composition and photoactivity to produce a clear, unambiguous view of the role of N-doping in these particular samples.

2. Experimental

2.1. Growth

An atmospheric pressure thermal CVD coater was used to grow thin films of TiO_2 on glass substrates [Saint Gobain], which possessed a barrier coating of SiO_2 to prevent diffusion of impurities from the glass. The precursors used were titanium tetrachloride and ethyl acetate (both from Aldrich), which were transported through the reactor by a carrier gas of nitrogen. The concentrations used were 4.9×10^{-4} and 3.65×10^{-3} mol/min, respectively. The N-dopant was ammonia (BOC), which was accurately metered by a mass-flow-controller. The growth conditions, which were varied, are shown in Table 1. The total gas flow rate was $10\,l\,min^{-1}$. Note that great care was needed with the addition of NH_3 to $TiCl_4$ as these reagents react readily to form a solid adduct [43], which could lead to equipment blockages as well as preventing addition of N to the TiO_2 within a transparent film. To reduce the chances of this occurring the NH_3 was added just before the reactor baffle and all lines were heated to prevent precursor accumulation. Interestingly the other commonly used titanium precursor, titanium tetraisopropoxide, is generally considered to contain too much oxygen, and so favours production of just the oxide rather than the oxynitride [44].

2.2. Characterisation

Standard techniques of X-ray diffraction (Siemens D5000), micro-Raman 514.5 nm Ar line (Renishaw 1000), UV/vis spectroscopy (Hewlett Packard HP895A) and SEM (Philips XL30) were used to characterise the samples. Film thickness was esti-

Table 1
Growth conditions employed for the growth of N-doped TiO_2 films together with the film thicknesses as estimated from the colour fringes

Sample number	Ammonia flow (sccm)	Growth time (s)	Substrate temperature (°C)	Layer thickness (nm)
N1	188	40	650	40
N2	188	80	650	80
N3	188	80	757	130
N4	188	80	650	80
N5	148	80	650	60
N6	108	80	650	100
N7	88	80	650	120
N8	188	80	700	120
N9	188	80	600	130

mated by relating the reflected colour to a calibrated chart for thickness versus refractive index. This method (and chart) is routinely used within the glass industry and shown by our own cross-checks to be accurate. X-ray photoelectron spectroscopy, XPS (Kratos AXIS Ultra) with an Al (monochromated) Kα radiation source was used to check for the presence of N and valence band measurements. It was necessary to use a charge neutraliser as all the samples were insulating. This tends to shift the peak positions by about 2 eV so both composition and bandgap measurements are referenced to the residual C 1s signal at 285 eV. Curve fitting used CASA XP software using a mixture of Gaussian–Lorentzian functions to deconvolute spectra. To test the photocatalytic behaviour under UV (365 nm) and visible (>400 nm) the degradation of stearic acid was followed by FTIR (Bruker, Vector 22).

3. Results and discussion

The films were all transparent and varied in thickness from approximately 40 to 130 nm, as judged by the colour fringes, see Table 1. A yellowish tinge, which has previously been taken to imply the presence of the oxynitride [23,33,38], could be seen on all samples. They generally increased in thickness with decreasing NH_3 input and increasing growth temperature. To overcome the problems of very weak XRD signals a glancing angle set-up was used, which led to acceptable results, Fig. 1.

From Fig. 1 it can clearly be seen that all the samples contained anatase (JCPDS data base 21-1272) but only sample N2 (red trace) shows very weak additional peaks at 18 and 33° that may relate to the presence of a true oxynitride (JCPDS data base $TiO_{0.34}N_{0.74}$). It can also be seen that for our samples, there was no sign of any peaks relating to TiN, which would appear at 36.6 and 42.6° (JCPDS data base 38-1420) or rutile (JCPDS data base 21-1276).

This result is in good agreement with most other researchers who, at low doping levels, see no sign of any other peaks than those of TiO_2 for their 'visibly active' samples, although Suda et al. [31] show a series of samples of different N concentration,

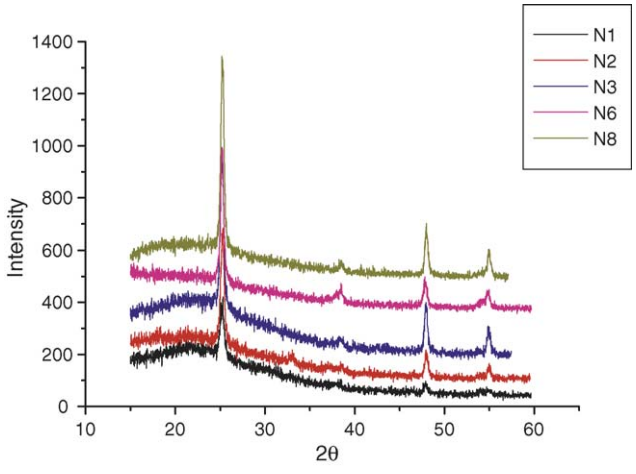

Fig. 1. A selection of the XRD data obtained from TiO_2 films grown in the presence of NH_3 in the process gas.

which show anatase and/or TiN. From these data and XPS data Suda et al. conclude that they have TiO_xN_y. This conclusion was based on the observation that the Ti 2p XPS feature consisted of a broad multiple peak which these authors attribute to a mixture of TiO_2 at a higher binding energy than expected 460 eV (rather than 458.3 eV), possibly due to N incorporation, together with some TiN. Unfortunately, in this work, no figures are presented as to the extent of N incorporation in the film. Other papers dealing with mainly TiN with relatively small amounts of O show a possible TiO_xN_y phase at ca. 41 at.% O, although citing the fact that the samples were of low crystallinity with broad peaks [45] while another assumes the peak at 36.6° is for the oxynitride rather than TiN [37] despite the fact that this assumption could only be valid for very high N concentrations. Again, in this latter study, there was no unambiguous measure of the extent of N incorporation. Indeed this assignment is rather questionable, since it might be expected that the 'TiN' peak at 36.6° should move to higher 2θ values as more O substitutes for N (ionic radius of O being smaller than that of the N) [46].

Variation in diffracted intensity will relate to either to changes in crystallinity or to film thickness. Only a small variation in intensity (4× maximum change) was observed for most of the samples with N1, N2 and N6 having the lowest intensity. The exception to this was sample N9, which gave rise to the highest diffracted intensity recorded from this series of samples.

This sample was grown at a lower temperature (600 °C) and is a similar thickness (130 nm) to samples N3 and N8, which were grown at higher temperatures (757 and 700 °C, respectively). All other conditions were identical and so it is most likely that the improved crystallinity must relate to the lower growth temperature, the higher temperatures leading to a loss of crystallinity, albeit for an equivalent growth rate. However, the equivalent sample grown at 650 °C (N2) and lying between those of N9 and N8 (700 °C) does not fit within this trend. It is much thinner (80 nm) and hence implies a much lower growth rate. Even if of similar crystallinity would be likely to have lower intensity signals. From evidence produced later within this paper the much slower growth rate is considered due to the incorporation of nitrogen.

Raman spectroscopy (Fig. 2) confirmed that the samples all contained anatase with no sign of any features due to rutile or other materials. It was noticeable that far more accumulations and longer exposure times were required in order to obtain data for these samples as compared to the undoped TiO_2 samples of similar thicknesses. This suggests that the samples were less crystalline, particularly when large amounts of NH_3 were added.

The Raman spectra all show the standard features of anatase at 393.9, 513.2 and 636.3 cm^{-1} corresponding to the B_{1g}, $B_{1g} + A_{1g}$ and E_g mode symmetries [47]. Here the B_{1g} mode relates to O–Ti–O bending type vibrations while the others to Ti–O stretching type vibrations [48].

SEM micrographs of the films grown in the presence of NH_3 films look very different from those grown without NH_3 in the process gas, Fig. 3 (Fig. 3e is the SEM image obtained from a nominally undoped film of thickness 80 nm). The films grown with the highest NH_3 flows appear less structured, in that the well-defined crystallites depicted in Fig. 3e are not observed in

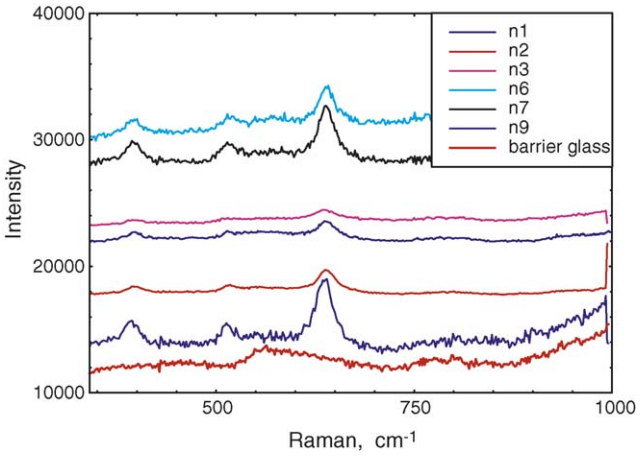

Fig. 2. Raman spectra of a selection of deposited films.

the presence of ammonia. Thus it may be that the films grown in the presence of ammonia contain more amorphous material although this cannot be confirmed directly by SEM.

Similar changes in growth morphology, with NH_3 concentration have been reported by Pradhan [37] although the films deposited are stated to be a mixture of TiO_2 (rutile) and TiO_xN_y (XRD peak at $2\theta = 36.6^\circ$, assumed to be oxynitride rather than TiN by the authors). The formation of rutile opposed to anatase may relate to the use of an alternative titanium precursor (titanium tetra isopropoxide) and low pressure.

Characterisation using UV/vis spectroscopy (Fig. 4) shows that there was no large shift in the position of the main peak (315 ± 2 nm) for samples grown in the presence of NH_3 as compared to the position of the peak in the spectrum obtained from a nominally undoped sample of similar thickness (316 ± 2 nm). Thus there is no evidence of any change in the position of the

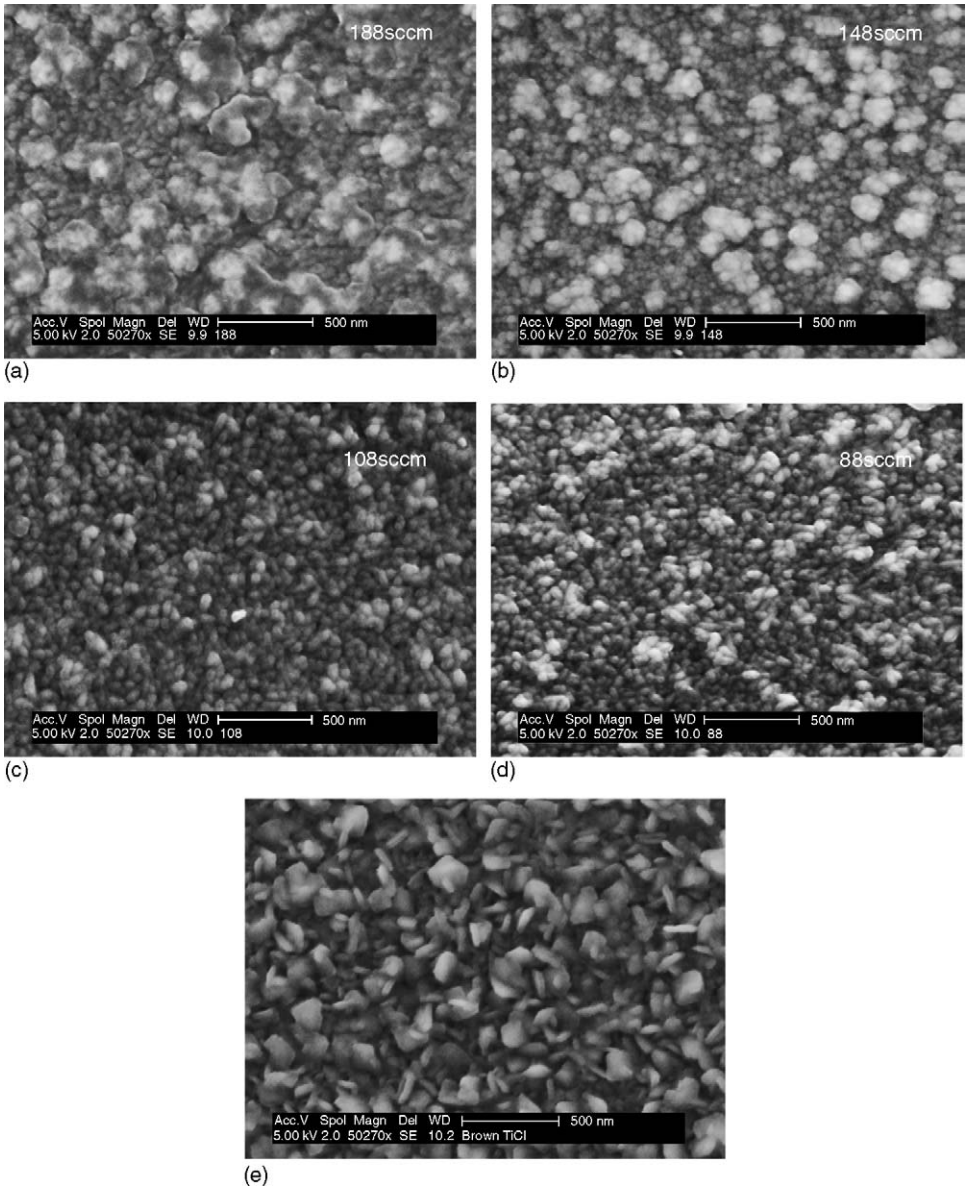

Fig. 3. SEM images of films grown under different NH_3 flow rates: (a) 188 sccm NH_3, 80 nm thick; (b) 148 sccm, 60 nm thick; (c) 108 sccm, 100 nm thick; (d) 88 sccm, 120 nm thick; (e) undoped TiO_2 film of thickness ca. 80 nm.

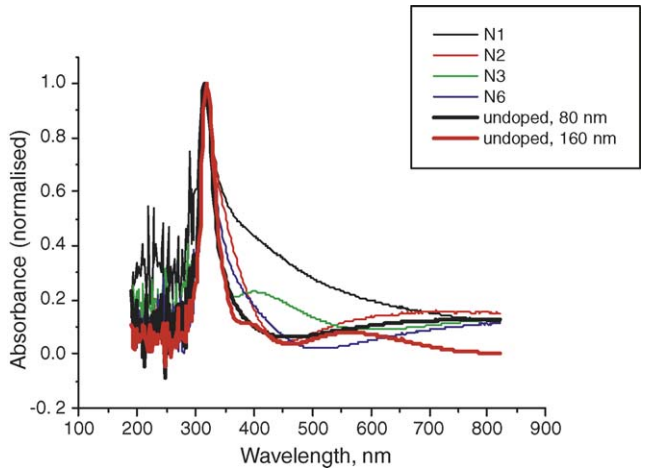

Fig. 4. UV/vis absorption spectra measurements of some of the N-doped TiO_2 samples, together with the spectrum recorded from two nominally undoped samples (heavy black line and heavy red line).

main absorption edge, although this would not be expected for small changes in composition. The appearance of a peak, rather than an edge, is due to removal of the background from the glass substrate (so only the effect of the TiO_2 film is seen) and the uncorrected spectral response of the spectrometer.

In contrast, large shifts were seen by Suda et al. [31], but this was for samples of very high N content, as judged from the XPS. Unfortunately, no figures for the levels of N incorporation were given in the paper, but the Ti 2p XPS shown confirms presence of peaks for TiO_2 and TiN. Other papers (for <1% N) show broadening to higher wavelength [18,19,34], which is related to doping. From Fig. 4 it may be seen that for three of the samples grown in the presence of NH_3, namely N1, N2 and N6, the spectrum shows a distinct broadening towards longer wavelengths which would be consistent with these previous studies if these samples were to contain incorporated nitrogen [18,19,34]. Fig. 4 also reveals that the spectrum for sample N3 (green trace), which was grown at the highest temperature employed in these experiments (757 °C), has an additional broad peak at 405 nm. Like the peak broadening referred to above, an additional peak at higher wavelength (450 nm) has previously been used as evidence that the nitrogen has been successfully incorporated as a dopant [23], despite a lack of evidence for this from XPS (N 1s) measurements, presumably because the levels of N incorporation were below the detection limits for XPS.

Thus it would seems that for samples grown at a temperature of ca. 650 °C in the presence of NH_3 some broadening of the main peak to longer wavelengths is observed which may be due to N incorporation. Similarly, for the sample grown at the higher temperature of 757 °C in the presence of NH_3, a new feature appears which could also arise from N incorporation. However, although broadening to higher wavelength and these additional peaks can be related to doping there is another possibility. With sufficient refractive index contrast (between substrate and film) and a uniform film it is possible to get Fabry–Perot interference. Depending on the period of the oscillations (related to film thickness) and spectrometer resolution this could lead to additional peaks and/or broadening of the main peak.

Fig. 4 also shows UV/vis absorption spectra obtained from two nominally undoped films. The undoped sample spectrum depicted as the heavy black line effectively tracks the spectrum obtained for sample N3, apart from the lack of the additional feature near 405 nm. However the undoped sample spectrum depicted as the heavy red line shows clear signs of both broadening and an additional feature at longer wavelengths.

Thus we conclude that the presence of broadening and/or the appearance of additional longer wavelength features does not correlate directly with N incorporation and as such arises via Fabry–Perot interference. This is an important point for experiments of this nature, since it demonstrates the fallibility of using UV/vis absorption spectroscopy alone to detect changes in band structure.

In order to provide a definitive answer as to whether N was incorporated XPS was used. As noted earlier, of all the samples grown only three produced the N 1s peak at 396 eV, which is attributed to atomic β-substituted N [49]. These were samples N1, N2 and N6 (Fig. 5). Samples N1, N2 and N6 were grown at 650 °C, under N_2 with flow rates of NH_3 in excess of 100 sccm. Thus it would be tempting to identify these parameters as those required in order to achieve β-substituted atomic N.

However, if one examines the conditions depicted in Table 1, this would then raise questions as to why other samples grown in the presence of NH_3, and in particular samples N4 and N5, did not yield the feature in question in the XPS. In order to try to address this inconsistency, it is first necessary to consider further the nature of the XPS data obtained from those samples that appear to contain nitrogen.

For samples N1, N2 and N6 XPS spectra obtained showed no evidence of any signal at 397 eV, which has previously been

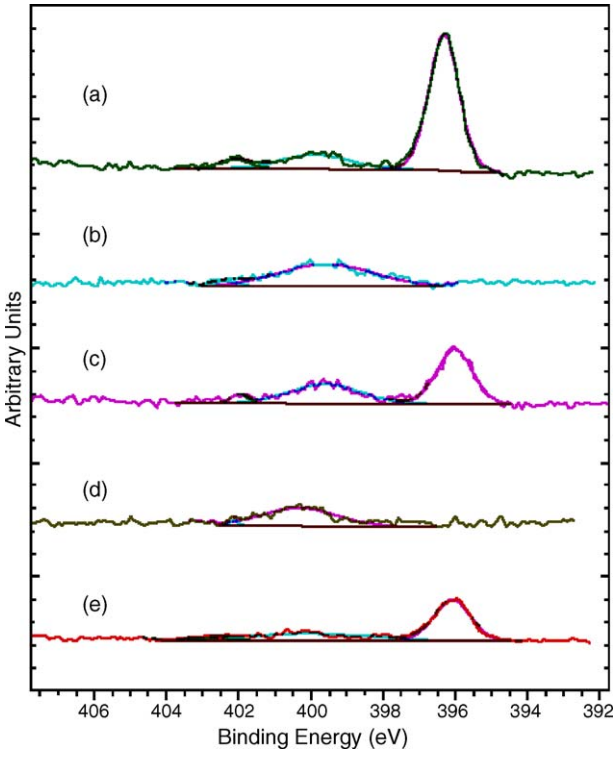

Fig. 5. N 1s XPS of the films: (a) N1; (b) N3; (c) N2; (d) undoped film; (e) N6.

assigned to N^{3-} (TiN) [50,51]. The N 1s spectra all showed other fairly weak (and hence noisy) signals at 400 and 402 eV which have been assigned to molecular, chemisorbed N2 [17,19,28,49], NH_x species located in interstitial sites (399.6 eV) [52], NO_x (or NH_x) (400 eV) [23,35], or an oxynitride (399.3 eV) of stoichiometry equivalent to $TiN_{0.5}O_{0.5}$ [53]. For the samples prepared in this work, this latter oxynitride compound can be ruled out, since the XPS peak would be considerably more intense if there were a 1:1 stoichiometry between N and O. Also, for the oxynitride compound there would be strong Ti 2p signals relating to the different chemical species, which is not the case here as will be discussed in more detail below. It is important to note that samples grown without addition of any N precursor also showed this signal. As an example the XPS data for a thin, colourless film is also shown in Fig. 5d. Here it can be seen that there is still signals round 400 eV, but as expected no signal at 396 eV for the substitutional nitrogen. A similar result for an undoped sample was seen by Morikawa et al. [34], although this observation was not commented on. As the signal is also seen in undoped samples, grown in a carrier gas of N_2, we assign this signal to trapped molecular N_2.

Further XPS analysis established that the incorporation of N only extended to the first 3 cm of the substrate (along the flow path of the gases into the reactor) indicating that the reaction occurred almost as soon as the reactants entered the reactor. This result is suggestive of the involvement of the high chemical affinity known to exist between $TiCl_4$ and NH_3. Curve fitting analysis was performed on the spectra that displayed the XPS peak at 396 eV. If it is assumed that this feature does indeed represent incorporated N, then the curve fitting analysis suggests levels of incorporation of between 1.5 and 5 at.%, Table 2.

The O 1s XPS scan confirmed the presence of O^{2-} attached to Ti^{4+} at 530.3 eV, along with a peak at 531.6 eV, which is assigned to absorbed water [54].

Most previous reports relating to N-doped TiO_2 for visible light activity where XPS was also used, although addressing the nature of the N 1s XPS feature, do not make mention of the corresponding Ti 2p XPS data. Previous research into the nature of the Ti 2p signal has focussed upon either TiN or high N containing oxynitrides [29,50,51,55]. These all show the presence of at least two distinct Ti species, relating to the TiO_2 and TiN components. Suda et al. [31] reasoned that a shift from 460 to 458.3 eV of the Ti $2p_{3/2}$ relates to N incorporation (although this work also showed additional Ti 2p signals relating to TiN). In this present work, the high resolution Ti 2p XPS data (Fig. 6) showed only the presence of one distinct species of titanium—that of Ti^{4+} attached to O^{2-} at 458 eV ($2p_{3/2}$) [54]. The main peak positions for the doped and undoped samples are similar so there is no major change in chemical environment for the titanium.

Table 2
β-Substitutional N within titanium dioxide

Sample	% incorporated N
N1	4.59
N2	2.13
N6	1.47

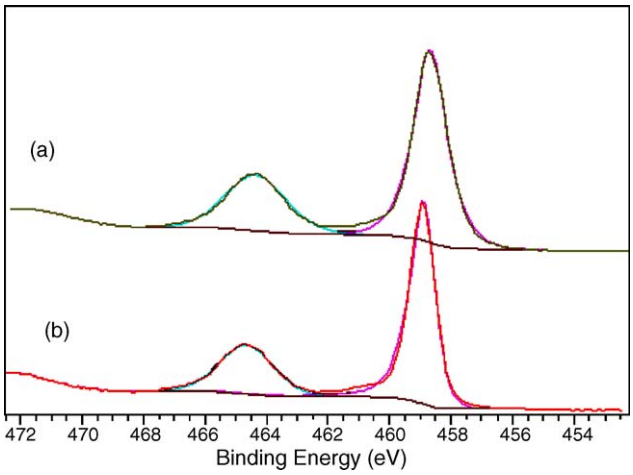

Fig. 6. High resolution XPS for Ti 2p for: (a) N-doped TiO_2 (N1); (b) TiO_2.

Fig. 6 shows the Ti 2p spectra for both a doped and undoped sample grown by the same method and of a similar thickness. At the very low levels of incorporated N little change would be expected. There was no obvious sign of any peaks at 455.2 eV, which would relate to TiN [49]. However, according to the literature [56] there is a small peak at 457.4 eV, relating toTi^{3+}, which maybe contributing to the peak broadening. To check if this species might be present in our samples, additional curve fitting peaks were added using constraints for area and position ($2p_{3/2}$ relative to $2p_{1/2}$), but we could only fit reasonable values for the sample of lowest N content (N6) giving ca. 4% Ti^{3+} (of the total Ti present) at 457.58 eV. For the other samples no reasonable fit could be obtained as their Ti 2p peaks tended towards that of the maximum constraint values of 548 eV (or those of the Ti^{4+} if no constraints) along with poorer fit values (i.e. residual standard deviation).

The Ti 2p signals showed a broadening (as measured from the full width at half maximum peak height) due to the β-N with values between 1.03–1.3 eV ($2p_{3/2}$) and 0.74–0.87 eV for non-doped samples. This may be also due to an increase in disorder or defect structure [50]. The values for the non-doped samples compare well with much thinner, highly crystalline commercial TiO_2 samples, e.g. the peak position recorded from a sample of the St Gobain product Bioclean^{TM} was 0.86 eV. However, in terms of possible disorder-induced broadening, by comparison with the work of Prieto and Kirby [50] it is concluded that our undoped samples were not particularly disordered. For comparison, in the work of Prieto et al., a disordered sample gave rise to a line broadening on the order of 1.62 eV opposed to 1.20 eV for a 'good' (presumably highly crystalline) sample [50]. It is therefore concluded that the line broadening of 1.03–1.3 eV observed for our doped samples represents samples that possess some considerable order, although this is certainly less than the order present in the undoped samples.

To confirm the validity of the XPS curve fit Rutherford Backscattering was performed on samples N1 and N2. For sample N1 the 4% value was confirmed, with the RBS showing a small signal for N and a corresponding dip in the O rising edge. For sample N2 no N was detected, but from the modelling it was

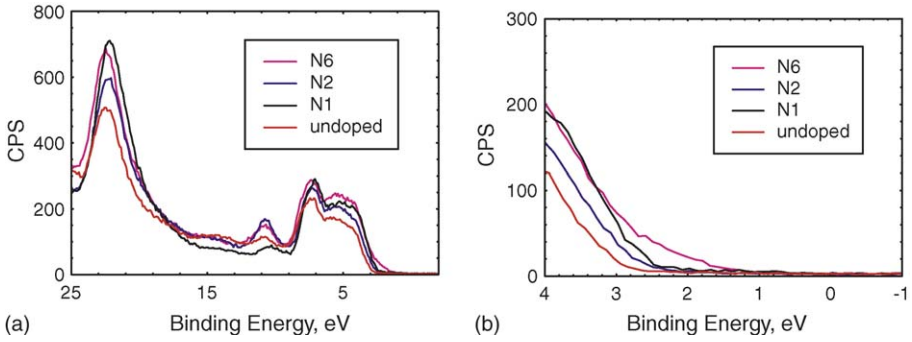

Fig. 7. (a) Valence band spectra of doped samples; (b) near Fermi level bandgap of N1 (black), N2 (blue), N6 (pink), undoped 40 nm (red).

obvious that the sensitivity of the RBS was not high enough to detect less than ca. 2% N. The problem here arises mainly due to the large O background from the glass substrate and TiO_2 film masking such small signals.

XPS was also used to study the valence band structure for samples N1, N2 and N6 (Fig. 7). All the samples show the same major features which are assigned to O 2s (23 eV), adsorbates such as OH or CO (10.8 eV), O 2p σ-bonding (7.4 eV) and O 2p π-bonding (5.4 eV) [56]. The Ti 3p state is at 37.3 eV (not shown in Fig. 7a) for both the doped and undoped samples. If there were any sign of Ti^{3+} defect states they would be located near the Fermi level (round 0.8 eV) [57]. No sign of this signal is seen, even for sample N6 (which is considered to contain a low amount of Ti^{3+}). However, N6 does seem to tail off at energies closer to the Fermi edge than for the other samples. Unfortunately, XPS lacks the resolution required for low-level detection (use of synchrotron radiation is more common for this type of study), and this, coupled with the low X-ray photoelectron cross sections in the valence band region makes it particularly difficult to observe these defect states [58].

Fig. 7b shows the region of the bandgap near the Fermi level. It can be seen that the peak is broadest for the more highly doped samples as compared to the undoped samples. This would suggest that there is more electron emission near the edge with the doped samples.

Thus, for samples N1, N2 and N6 the XPS data is strongly suggestive of the existence of β-N incorporation, while there is little direct evidence of the existence of Ti^{3+} defect states in these samples.

Since the XPS data clearly indicated the presence of β-N incorporation for samples N1, N2 and N6, these samples were then analysed as to their photocatalytic activity. However, before these results are discussed it is necessary to return to the question of why other samples grown at similar temperatures and using similar quantities of NH_3, did not yield the necessary XPS features. At present we do not have a definitive explanation for this obvious inconsistency in our data other than to note that firstly, it is possible that there was indeed N incorporation in these samples but at levels that were below the limits of detection by XPS. Secondly, given that under the conditions employed reaction was observed to occur at the leading edge of the substrate, with the N incorporation localised into a very narrow region of the substrate. Due to this, it would be quite possible to take samples for analysis from areas where incorporation was not favoured and thus obtain misleading data. This said, we accept that as a result of these uncertainties, we cannot define the exact parameters by which it is possible to directly incorporate nitrogen into the growing TiO_2 film. However, we believe that the results obtained for samples N1, N2 and N6 are likely to point the way towards these conditions, but that more control is needed over gas mixing and flow conditions before these can be fully confirmed as the necessary parameters. While this is a little disappointing, it is typical of a CVD process which may be dramatically influenced by a wide range of parameters some linked directly to equipment design. Despite this uncertainty, having obtained samples, which do show N incorporation, we have been able to assess these for photocatalytic activity in both the visible and the UV, which was the primary purpose of these studies.

The samples that did contain β-N were tested for photoactivity using the stearic acid test described earlier, using both a xenon arc lamp (75 W) and a household security light (300 W) with a 400 nm cut off filter specifically designed to remove all photons of wavelength less than 400 nm, to see if the addition of the β-N allowed the films to degrade contaminants when irradiated with visible light only. Emission spectroscopy was used to check the energy range of the lamps and the effectiveness of the filter. Contact angle measurements were also carried out but they proved to be inconclusive. Fig. 8 shows the results for photoactivity testing in the visible light region using the Xe arc lamp. The results are then summarised in Table 3.

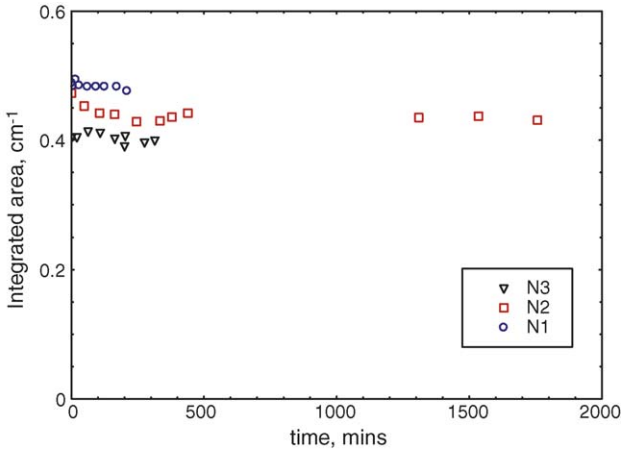

Fig. 8. Graph of integrated area under the stearic acid C–H stretching peaks (wavenumber range = 2980–2820 cm^{-1}) of stearic acid against time.

Table 3
Summary of the visible light photoactivity testing results for both doped and undoped samples

Sample	Light source	Activity rate (cm^{-1} min^{-1})
N1	Xe arc lamp	5.86E−5
N2	Xe arc lamp	4.28E−5
N3	Xe arc lamp	4.64E−5
N6	Security lamp	1.83E−5
Barrier glass	UV lamps	15E−5
Bioclean™	Fluorescent room light	15E−5

As can be seen from Fig. 8 and Table 3, there is little change in the concentration of stearic acid with time for any of the sample, even that of sample N2 which was tested to nearly 30 h. To attempt to see any activity in the visible light region a much more powerful lamp was tried with the sample containing the lowest level of N (N6, 1.5%), Fig. 9. This sample was chosen since the results presented earlier show quite clearly how the conditions used to incorporate higher levels of N also result in a severe degradation in morphology, which is likely to have a highly detriments effect on the photoactivity of any film. Thus the use of sample N6 represents a trade-off in that the sample does contain β-nitrogen, but at a level where the degradation in morphology is not particularly significant.

The result shown in Fig. 9 again indicates that no significant reduction in the amount of stearic acid occurred over the period of the experiment (over 30 h), clearly establishing that no visible light activity was detected, although there do appear to be some minor fluctuations of the integrated area. These may be due to the heat of the lamp affecting the stearic acid film, rather than any changes caused by the sample.

From these photocatalytic tests results it is apparent that there is no noticeable activity in the visible light region. This is particularly obvious when sample data are compared to reference values where no change is expected, such as with barrier glass. However, these samples were also tested using the standard stearic acid test conditions (365 nm UV light, activated and tested at 3 mW/cm^2) to determine if the activity had been completely diminished. The data presented in Fig. 10 establishes clearly

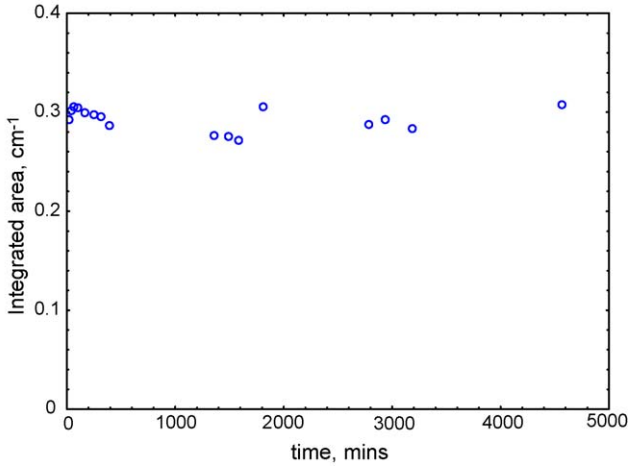

Fig. 9. Graph of integrated area of stearic acid against time.

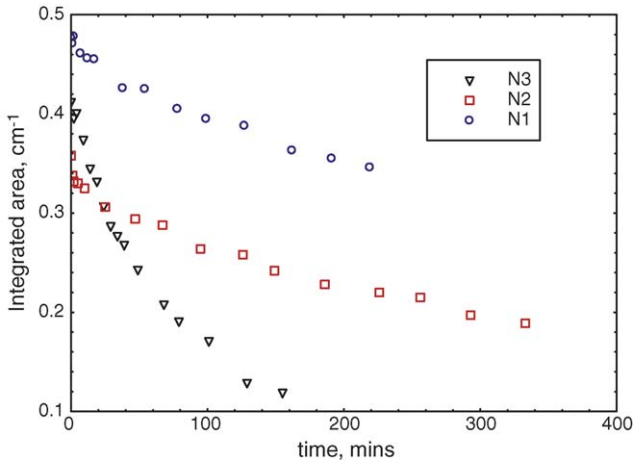

Fig. 10. UV activity of N-doped TiO_2 films.

that in contrast to the visible light activation experiments, the samples possessed noticeable activity when irradiated with UV light.

It can be seen that samples N1 and N2 have a much lower activity in the UV than sample N3, which although grown under similar conditions to those used for samples N1 and N2, did not yield the appropriate N XPS feature. The presence of ammonia during the growth process has clearly affected the UV photocatalytic activity of the nitrogen doped samples, while the higher temperatures employed during the growth of sample N3 not only may have helped to inhibit the incorporation of nitrogen, but also helped to maintain the crystallinity and morphology needed to sustain higher levels of photoactivity. This said, it is clear that the activity of sample N3 is still much lower than for undoped samples, as may be seen from the comparison of activities shown in Table 4.

Some reduction of the activity of the doped TiO_2 films in the UV has been previously reported [18,19,30], although most researchers do not mention whether doping has any effect in changing the UV activity, over that of the undoped samples. One possible explanation of the reduction in UV activity observed here is that annealing in a reducing atmosphere such as NH_3 may lead to oxygen depletion via water formation, which in turn results in an increase in either Ti^{3+} defects or oxygen vacancies. Oxygen vacancies in particular are known to act as electron–hole recombination centres and hence reduce photocatalytic efficiency [59].

Table 4
Calculated photocatalytic rates under UV (365 nm)

Sample	Photoactivity (cm^{-1} min^{-1}) (over 60 min)	Thickness (nm) (average)
N1	0.001	40
N2	0.001	80
N3	0.004	130
Colourless non-doped	0.006	40
Brown non-doped	0.005	80
Violet non-doped	0.011	120

4. Conclusions

Films of polycrystalline anatase have been grown by CVD using titanium tetrachloride and ethyl acetate in the presence of ammonia. Some films display absorption features, which extend towards the visible light region of the spectrum. However, since the spectra obtained from nominally undoped films also possess these features we suggest that N incorporation cannot be assumed on the basis of changes in the absorption spectroscopy. While some inconsistencies have been noted in terms of the precise CVD growth parameters that result in detectable levels of N incorporation as detected by XPS, it appears that a growth temperature in the region of 650 °C is necessary to facilitate N incorporation at levels of between 1.5 and 5 at.%. For selected samples, clear evidence of β-N incorporation has been obtained, while no direct evidence for the existence of Ti^{3+} defect states has been obtained.

Despite the presence of β-N incorporation and absorption spectra, which possess features extending towards the visible, no visible light-induced photocatalytic activity has been observed whatsoever, while the conventional UV light-induced photoactivity of these films is severely reduced as compared to films grown in the absence of ammonia. Thus the presence of β-nitrogen alone cannot be cited as a means of inducing visible light activity in TiO_2 films.

Perhaps the most interesting finding of this work is that the morphology of the films is dramatically influenced by the addition of ammonia to the process gases, with the deposited film appearing less well defined in terms of the appearance of clearly defined crystallites. Since ammonia addition also reduces the growth rate, it is proposed that the surface chemistry of TiO_2 growth is strongly influenced detrimentally by the presence of ammonia.

These effects are believed to be directly related to the reduction in photocatalytic activity as measured under UV illumination, possible via the introduction of defects, which may act as charge carrier recombination centres.

Acknowledgements

This work was supported by EU Grant No. GRD1-2001-40791, PHOTOCOAT. The authors also wish to thank M. Faulkner at Manchester University Materials Science Centre for the SEM images produced in this paper and R. Valizaheh at MMU for the RBS.

References

[1] A. Mills, S. Lee, J. Photochem. Photobiol. A 152 (2002) 233–247.
[2] I.M. Arabatzis, S. Antonaraki, T. Stergiopoulos, A. Hiskia, E. Papaconstantinou, M.C. Bernard, P. Falaras, J. Photochem. Photobiol. A 149 (2002) 237–245.
[3] S.B. Kim, S.C. Hong, Appl. Catal. B: Environ. 35 (2002) 305–315.
[4] Y.H. Hsien, C.F. Chang, Y.H. Chen, S.F. Chang, Appl. Catal. B: Environ. 31 (2001) 241–249.
[5] M. Rosana, W. Alberici, F. Jardim, Appl. Catal. B: Environ. 14 (1997) 55–68.
[6] L. Xiao-e, A.N.M. Green, S.A. Haque, A. Mills, J.R. Durrant, J. Photochem. Photobiol. A 162 (2004) 253–259.
[7] http://www.pilkington.com.
[8] L. Cassar, MRS Bull. 29 (2004) 328–331.
[9] M. Simon, K. Hund-Rinke, I. Trick, A. Zastrow, EJIPAC, Saarbrucken, Germany, 2004.
[10] S.H. Lee, S. Pumprueg, B. Moudgil, W. Sigmund, Colloid Surf. B 40 (2005) 93–98.
[11] J.C.S. Wu, C.H. Chen, J. Photochem. Photobiol. A 163 (2004) 509–515.
[12] S. Hu, R.J. Willey, B. Notari, J. Catal. 220 (2003) 240–248.
[13] V. Keller, P. Bernhardt, F. Garin, J. Catal. 215 (2003) 129–138.
[14] T. Umebayashi, T. Yamaki, T. Sumita, S. Yamamoto, S. Tanaka, K. Asai, Nucl. Instrum. Meth. Phys. Res. Sect. B 206 (2003) 264–267.
[15] A. Fuerte, M.D. Hernandez-Alonso, A.J. Maira, A. Martinez-Arias, M. Fernandez-Garcia, J.C. Conesa, J. Soria, Chem. Commun. (2001) 2718–2719.
[16] I. Justicia, P. Ordejon, G. Canto, J.L. Mozos, J. Fraxedas, G.A. Battiston, R. Gerbasi, A. Figueras, Adv. Mater. 14 (2002) 1399–1402.
[17] R. Asahi, T. Morikawa, T. Ohwaki, K. Aoki, Y. Taga, Science 293 (2001) 269–271.
[18] M. Miyauchi, A. Ikezawa, H. Tobimatsu, H. Irie, K. Hashimoto, Phys. Chem. Chem. Phys. 6 (2004) 865–870.
[19] H. Irie, Y. Watanabe, K. Hashimoto, J. Phys. Chem. B 107 (2003) 5483–5486.
[20] Y. Sakatani, H. Koike, Japan Patent P2001-72419A (2001).
[21] O. Diwald, T.L. Thompson, T. Zubkov, E.G. Goralski, S.D. Walck, J.T. Yates, J. Phys. Chem. B 108 (2004) 6004–6008.
[22] M. Okada, Y. Yamada, P. Jin, M. Tazawa, K. Yoshimura, Thin Solid Films 445 (2003) 217–221.
[23] R. Nakamura, T. Tanaka, Y. Nakato, J. Phys. Chem. B 108 (2004) 10617–10620.
[24] I.N. Martyanov, U. Sitharaman, S. Rodrigues, K.J. Klabunde, Chem. Commun. (2004) 2476–2477.
[25] I. Nakamura, N. Nwgishi, S. Kutsuna, T. Ihara, S. Sugihara, K. Takeuchi, J. Mol. Catal. A 161 (2000) 205–212.
[26] S.M. Prokes, J.L. Gole, X. Chen, C. Burda, W.E. Carlos, Adv. Funct. Mater. 15 (2005) 161–167.
[27] W. Choi, A. Termin, M.R. Hoffann, J. Phys. Chem. 98 (1994) 13669–13679.
[28] O. Diwald, T.L. Thompson, E.G. Goralski, S.D. Walck, J.T. Yates, J. Phys. Chem. B 108 (2004) 52–57.
[29] J. Guillot, F. Fabreguette, L. Imhoff, O. Heintz, M.C. Marco de Lucas, M. Sacilotti, B. Domenichini, S. Bourgeois, Appl. Surf. Sci. 177 (2001) 268–272.
[30] P. Frach, D. GloB, M. Vergohl, F. Neumann, K. Hund-Rinke, EJIPAC, Saarbrucken, Germany, 2004.
[31] Y. Suda, H. Kawasaki, T. Ueda, T. Ohshima, Thin Solid Films 453/454 (2004) 162–166.
[32] A. Mills, S. Hunte Le, J. Photochem. Photobiol. A 108 (1997) 1–35, and references within.
[33] D. Li, H. Haneda, S. Hishita, N. Ohashi, Mater. Sci. Eng. B: Adv. Publ. Dec. (2004).
[34] T. Morikawa, R. Asahi, T. Ohwaki, K. Aoki, Y. Taga, Jpn. J. Appl. Phys. 40 (2001) L561–L563.
[35] S.M. Oh, T. Ishigaki, Thin Solid Films 457 (2004) 186–191.
[36] H. Noda, K. Oikawa, T. Ogata, K. Matsuki, H. Kamada, Nippon Kagaku Kaishi 8 (1986) 1084–1090.
[37] S.K. Pradhan, P.J. Reucroft, J. Cryst. Growth 250 (2003) 588–594.
[38] B. Kosowska, S. Mozia, A.W. Morawski, B. Grzmil, M. Janus, K. Kalucki, Sol. Energy Mater. Sol. Cells, Adv. Publ. Dec. (2004).
[39] A. Mills, J. Wang, J. Photochem. Photobiol. A 127 (1999) 123–134.
[40] P. Sawunyama, L. Jiang, K. Hashimoto, J. Phys. Chem. B 101 (1997) 11000–11003.
[41] Y. Paz, Z. Luo, L. Rabenberg, A. Heller, J. Mater. Res. 10 (1995) 2842–2848.
[42] A. Mills, G. Hill, S. Bhopal, I.P. Parkin, S.A. O'Neill, J. Photochem. Photobiol. A 160 (2003) 185–194.
[43] R. Gordon, J. Non-Cryst. Solids 218 (1997) 81–91.

[44] S.R. Kurtz, R.G. Gordon, Thin Solid Films 140 (1986) 277–290.
[45] F. Vaz, P. Cerqueira, L. Rebouta, S.M.C. Nascimento, E. Alves, P. Goudeau, J.R. Riviere, K. Pischow, J. de Rijk, Thin Solid Films 447 (2004) 449–454.
[46] F. Fabreguette, L. Imhoff, J. Guillot, B. Domenichini, M.C. Marco de Lucas, P. Sibillot, S. Bourgeois, M. Sacilotti, Surf. Coat. Technol. 125 (2000) 396–399.
[47] R. van de Krol, A. Goossens, J. Vac. Sci. Technol. A 21 (2003) 76–83.
[48] T. Ohsaka, F. Izumi, Y. Fujiki, J. Raman Spectrosc. 7 (1978) 321–324.
[49] N.C. Saha, H.G. Tompkins, J. Appl. Phys. 72 (1992) 3072–3079.
[50] P. Prieto, R.E. Kirby, J. Vac. Sci. Technol. A 13 (1995) 2819–2826.
[51] I. Milosev, H.H. Strehblow, B. Navinsek, M. Metikoshukovic, Surf. Interf. Anal. 23 (1995) 529–539.
[52] S. Souto, F. Alvarez, Appl. Phys. Lett. 70 (1997) 1539–1541.
[53] J. Halbritter, H. Leiste, H.J. Mathes, P. Walk, Fresen. J. Anal. Chem. 341 (1991) 320–324.
[54] Y.J. Sun, T. Egawa, L.Y. Zhang, X. Yao, Jpn. J. Appl. Phys. 41 (2002) L1389–L1392.
[55] D.H. Lee, Y.S. Cho, W.I. Yi, T.S. Kim, J.K. Lee, H.J. Jung, Appl. Phys. Lett. 66 (1995) 815–816.
[56] R. Sanjines, H. Tang, H. Berger, F. Gozzo, G. Margaritondo, F. Levy, J. Appl. Phys. 75 (1994) 2945–2951.
[57] R.L. Kurtz, R. Stockbauer, T.E. Madey, E. Roman, J.L. de Segovia, Surf. Sci. 218 (1989) 178–200.
[58] P.M.A. Sherwood, in: D. Briggs, J.T. Grant (Eds.), Surface Analysis by Auger and X-ray Photoelectron Spectroscopy, IMPubl, Chichester, 2003, pp. 531–555.
[59] S. Takeda, S. Suzuki, H. Odaka, H. Hosono, Thin Solid Films 292 (2001) 338–344.